Article

Identification and characterization of microRNAs during retinoic acid-induced regeneration of a molluscan central nervous system

Sarah E. Walker, Gaynor E. Spencer, Aleksandar Necakov and Robert L. Carlone *

Department of Biological Sciences, Brock University, St. Catharines, Ontario Canada L2S 3A1;
sw10tn@brocku.ca (S.W.); gspencer@brocku.ca (G.E.S.); anecakov@brocku.ca (A.N.)

* Correspondence: rcarlone@brocku.ca; Tel.: +1-905-688-5550

Abstract: Retinoic acid (RA) is the biologically active metabolite of vitamin A and has become a well-established factor that induces neurite outgrowth and regeneration in both vertebrates and invertebrates. However, the underlying regulatory mechanisms that may mediate RA-induced neurite sprouting remain unclear. In the past decade, microRNAs have emerged as important regulators of nervous system development and regeneration, and have been shown to contribute to processes such as neurite sprouting. However, few studies have demonstrated the role of miRNAs in RA-induced neurite sprouting. By miRNA-Sequencing analysis, we identify 482 miRNAs in the regenerating CNS of the mollusc *Lymnaea stagnalis*, 219 of which represent potentially novel miRNAs. Of the remaining conserved miRNAs, 38 show a statistically significant up or downregulation in regenerating CNS as a result of RA treatment. We further characterized the expression of one neuronally-enriched miRNA upregulated by RA, miR-124. We demonstrate for the first time that miR-124 is expressed within the cell bodies and neurites of regenerating motorneurons. Moreover, we identify miR-124 expression within the growth cones of cultured ciliary motorneurons (Pedal A), whereas expression in the growth cones of another class of respiratory motorneurons (RPA) was absent *in vitro*. These findings support our hypothesis that miRNAs are important regulators of retinoic acid-induced neuronal outgrowth and regeneration in regeneration-competent species.

Keywords: Retinoic acid, microRNA, RNA sequencing, neuronal regeneration, growth cone, *Lymnaea*

1. Introduction

Following injury to the central nervous system (CNS), the ability of damaged neurons to repair and regenerate functional connections is limited in most species. Only a few vertebrates are able to regenerate lost or damaged CNS tissues and cell types, though numerous invertebrates possess this intrinsic ability of self-repair [1, 2]. Interestingly, many trophic and chemotropic factors that mediate neuronal outgrowth and connectivity in regeneration-competent species are highly conserved and functional in many vertebrates and invertebrates [3-5]. However, a thorough understanding of the molecular and biochemical mechanisms underlying the production and utilization of these factors that results in functional CNS regeneration is lacking.

One critical factor that has been suggested to play a role in CNS regeneration in many species is the vitamin A metabolite, all-*trans* retinoic acid (RA). RA signaling mediates neuronal outgrowth [6] and differentiation [7] during both CNS development and regeneration [8-10]. To exert such effects, RA binds to two classes of nuclear receptors, the retinoic acid receptors (RAR) and the retinoid X receptors (RXR). Following ligand binding, specific subtypes of these receptors typically heterodimerize to regulate the expression of genes that contribute to numerous processes associated with both neuronal development and regeneration [7]. Our understanding of the role of RA

46 signaling in CNS regeneration has come largely from studies on urodele amphibians, such as the
47 newt and axolotl [9, 11-13]. More recently, the role of specific microRNAs as post-transcriptional
48 regulators, both upstream and downstream of RA signalling in the regenerating CNS has become an
49 important area of investigation.
50   MicroRNAs (miRNAs) are conserved, non-coding RNAs that post-transcriptionally regulate
51 gene expression by directly binding to mRNAs to suppress their translation into functional proteins.
52 In the adult newt, miR-133a was identified by microarray analysis as being a critical regulator of
53 RARβ expression. [14,15]. When the expression of this miRNA was experimentally increased by
54 electroporation of a mimic, RARβ expression was downregulated and posterior ependymal tube
55 outgrowth from the cut spinal cord was inhibited [14]. Moreover, miR-133 has also been implicated
56 in the regulation of spinal cord regeneration in zebrafish [16]. However, no studies to date have
57 examined the role of miRNAs in RA-mediated CNS regeneration in any invertebrate species.
58   RA signalling was originally thought to be a vertebrate innovation, but has now been
59 demonstrated in some CNS regeneration-competent invertebrate species [17], such as the pond snail,
60 *Lymnaea stagnalis*. RA is found in the CNS of *Lymnaea stagnalis* [17], and induces neurite sprouting
61 and attractive growth cone turning in various neuronal cell types [10, 18]. Moreover, components of
62 the retinoid-signalling pathway, including RAR and RXR, are expressed in the growth cones and
63 mediate RA-induced chemotropic responses [19,20]. As *Lymnaea* CNS neurons can regenerate and
64 this can be enhanced by RA signalling, our aim here was to determine whether miRNAs play a role
65 in the regenerative response of this invertebrate CNS.
66   In this study, we identified miRNAs in the regenerating CNS of adult *Lymnaea* and discovered a
67 specific subset that were either up-regulated or down-regulated during RA-induced neurite
68 sprouting. We then examined the spatial and temporal patterns of expression of one of these
69 dysregulated miRNAs, miR-124. Interestingly, we found that miR-124 displayed similar expression
70 patterns in *Lymnaea* as it does in many vertebrates. Specifically, we found miR-124 was enriched in
71 the adult CNS, and was upregulated during both development and CNS regeneration. Using *in situ*
72 hybridization, we also examined the spatial distribution of miR-124 in regenerating motorneurons
73 and demonstrated a cell-specific expression in regenerating growth cones.

74 **2. Results**

75 *2.1. miRNA-Sequencing analysis of miRNAs in the Lymnaea CNS*

76   As RA is capable of inducing neurite outgrowth from both vertebrate and invertebrate nerves,
77 the identification and functional characterization of miRNAs that might be involved in mediating
78 such retinoid-induced outgrowth was our primary focus. As a model system, we utilized adult CNS
79 from the regeneration-competent mollusc, *Lymnaea stagnalis*, whereby neurite sprouting from cut
80 nerves, as well as from individually cultured neurons, were examined.
81   The CNS of *Lymnaea* was removed from the animal by transecting all nerves emanating from
82 the CNS to the periphery. The CNS was incubated in either RA (10^{-5}M) or EtOH (0.1%; vehicle
83 control) for 72 hours, which was sufficient time for a regenerative response to occur. We found that
84 when dissected CNS were incubated in RA, the nerves exhibited robust neurite sprouting (Figure
85 1A), which did not occur in CNS incubated in EtOH alone (Figure 1B). Total RNA was isolated from
86 pooled samples of both RA-treated (regenerating/sprouting) and EtOH-treated (non-regenerating)
87 tissues 72 hours following treatment, and submitted for miRNA-Sequencing analysis.
88   The quality of our miRNA-Sequencing analysis was validated with appropriate length and
89 count distributions of the sequences and optimal phred scores, to ensure accuracy of the reads
90 (Figure 1C & D). The length distribution (Figure 1C) determined that the average length of our
91 mappable reads was ~22-23 base pairs, which is representative of the typical length of mature
92 miRNAs [21]. The phred scores identified the base call accuracy, and determined the probability of
93 an incorrect base reading. A perfect score of 40 corresponds to 99.99% accuracy of the reads, while a
94 score greater than 30 corresponds to 99.9% accuracy. Our data displayed typical phred scores of 38

95   and 39 (Figure 1D), suggesting a high accuracy (>99.9%) and providing confidence in our
96   RNA-Sequencing data analysis.
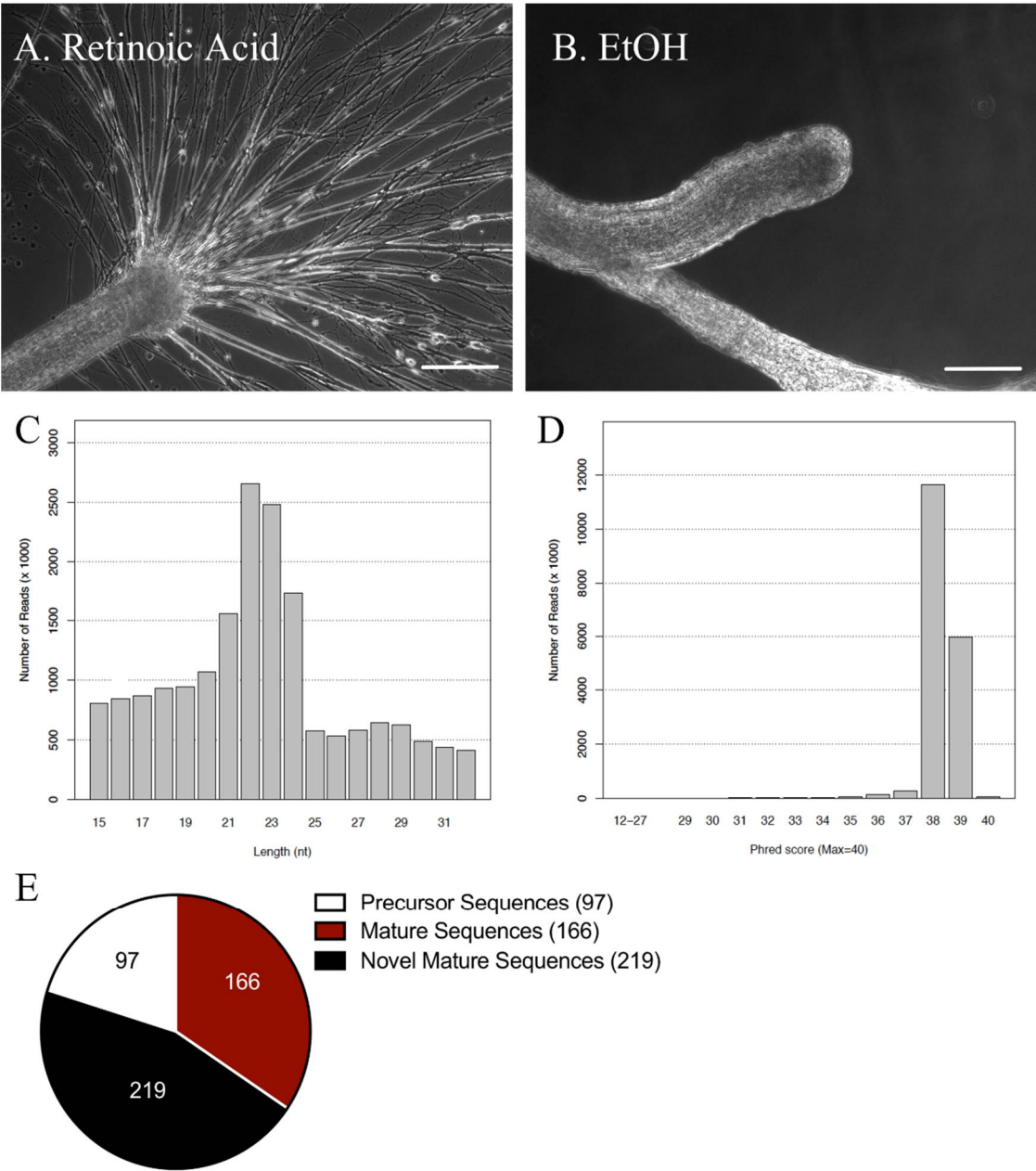
97   Total sequences: 482

98   **Figure 1.** miRNA-Sequencing data of regenerating *Lymnaea* CNS. **A & B**) Representative images of
99   regenerative outgrowth from cut nerves emerging from the *Lymnaea* CNS. Robust neurite outgrowth
100   is seen in CNS incubated in RA (**A**), though no outgrowth is seen from CNS incubated in EtOH
101   (vehicle control) (**B**). Scale bars=250 μm. **C**) Quality assessment of miRNA-Sequencing analysis using
102   the length and count distribution of sequences. Graph depicts the length distribution of reads
103   following the 3'adapter cut. Counts display a majority of reads in the range of 21-24 nucleotides,
104   corresponding to the length of mature miRNAs. **D**) Histogram of the average phred score per base in
105   a read after the 3'adapter cut. A phred score greater than 30 corresponds to an accuracy of 99.9%,
106   while a score of 40 represents an accuracy of 99.99%. **E**) Number of novel, mature and precursor
107   miRNAs identified in the *Lymnaea* CNS.

108   Mature miRNA sequence information in molluscs is currently very limited. At present,
109   miRBase release 22 (March 2018; http://www.mirbase.org/) reports the sequences of only three
110   molluscan species, *Lottia gigantia*, *Melibe leonina*, and *Haliotis rufescens*. To identify miRNAs in
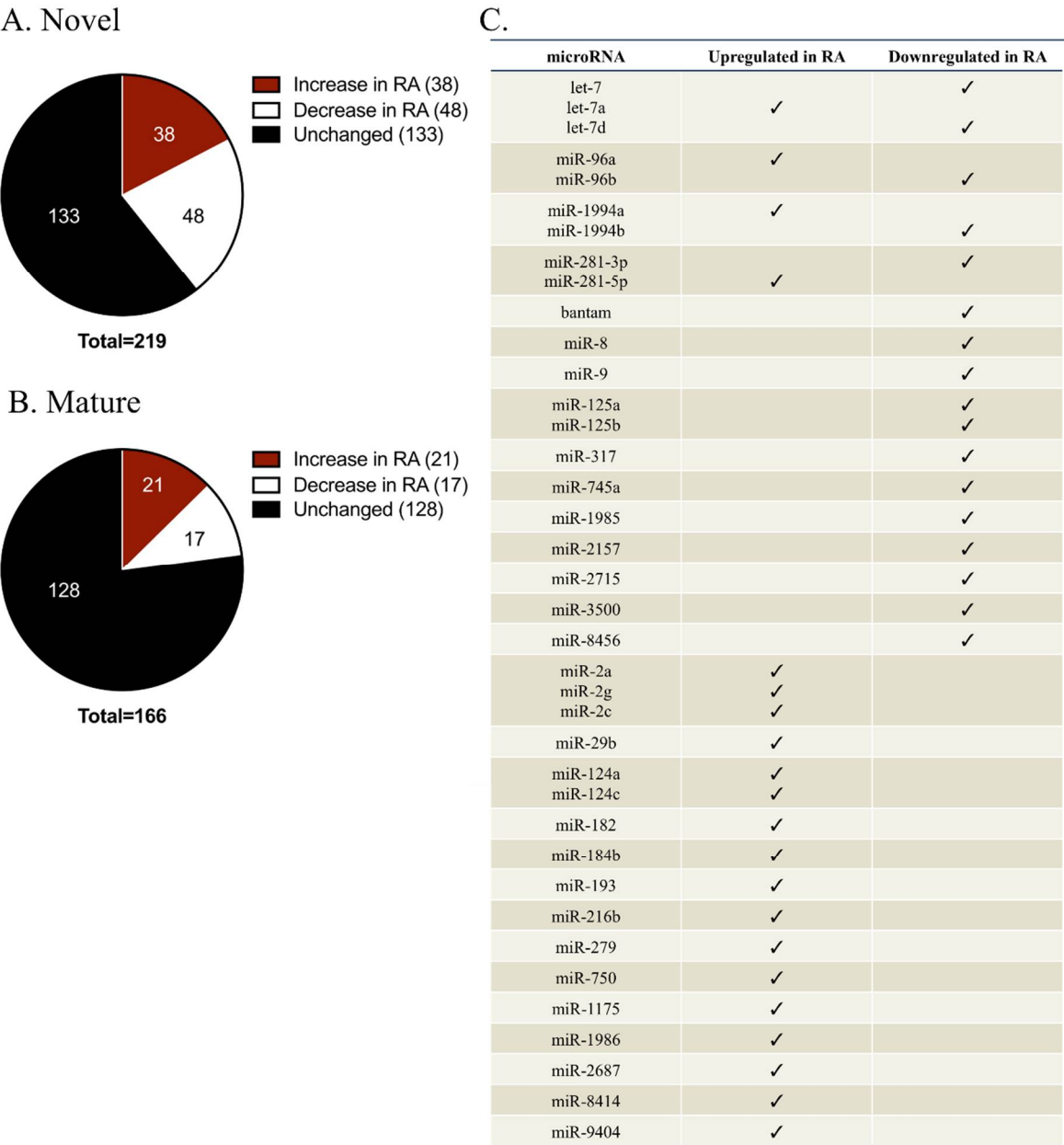
111 *Lymnaea*, the sequences generated from our miRNA-Sequencing analysis were matched to known
112 miRNAs in the mollusc, *Lottia gigantia*. The miRNA-Sequencing analysis identified 482 miRNA
113 sequences in the *Lymnaea* CNS, including 97 precursor miRNAs, 166 mature miRNAs and 219 novel
114 miRNAs (Figure 1E). The novel miRNAs represent a group of mature miRNAs that were not
115 matched to any other known species in miRbase. As most miRNAs are highly conserved, even
116 between distantly related species such as invertebrates and vertebrates [22], these novel miRNA
117 sequences may be *Lymnaea*-specific miRNAs, or possibly, miRNAs that have not yet been identified
118 or sequenced in other species. It is also possible that some of these novel miRNAs represent RNA
119 fragments.

120 *2.2. Identification of miRNAs that were differentially regulated during RA-induced regeneration*

121 From our miRNA-Sequencing data, 219 putative novel sequences represented a large
122 proportion of total sequenced reads (~45%). Of these novel sequences, 38 exhibited at least a 2-fold
123 increase in RA-treated samples, while 48 displayed at least a 2-fold reduction (Figure 2A). However,
124 all of the differentially regulated novel sequences were of extremely low abundance, typically with
125 less than 10 sequence reads in the entire CNS. Due to their extremely low level of expression, we did
126 not investigate any novel sequences further.
127 We next chose to focus on mature miRNAs that had previously been identified in other species.
128 Of the 166 mature miRNAs, 21 sequences exhibited at least a 2-fold increase in RA-treated CNS,
129 while 17 miRNAs displayed at least a 2-fold reduction (Figure 2B, C). A literature examination of
130 many of these differentially-regulated miRNAs shed some light on their known roles, and many
131 were found to contribute to the formation and/or function of the nervous system (Table 1). Many of
132 these miRNAs also exhibited overlapping cellular functions, contributing to processes such as
133 tumorgenesis [23-30], differentiation [31-33], proliferation [34-38], apoptosis [39-42] and cell cycle
134 regulation [43,34,44]. A subset of the miRNAs was associated with nervous system-specific
135 processes, such as differentiation [45-49], lifespan [50], neurite guidance [51-53] or synaptogenesis
136 [54-56]. We were specifically interested in miRNAs known to contribute to neuronal differentiation
137 and/or axonal guidance, processes that are known to be regulated by RA [10,57]. One potential
138 candidate was miR-125b, which contributes to the development of a permissive environment for
139 axonal outgrowth in the injured CNS of axolotls [53]. However, this miRNA has not been shown to
140 contribute to RA-induced regeneration in any species, indicating it was not a good candidate for
141 further analysis.
142 Additional candidate miRNAs identified by our miRNA-Sequencing included miR-124 and
143 miR-9, both of which are enriched in the nervous systems of many species and contribute to
144 neuronal differentiation [45-49] and axonal guidance [51,52]. Importantly, both of these miRNAs are
145 upregulated by RA in human and mouse cell lines [47,58,59]. However, we found that miR-9 was
146 downregulated in RA-treated CNS (Figure 2C), indicating it may have distinct roles and responses
147 to RA in the snail, compared to vertebrates. As described in vertebrates, however, miR-124 was
148 upregulated in RA-treated *Lymnaea* CNS (Figure 2C). As miR-124 has been associated with neurite
149 outgrowth, not only in mammals [60], but also in amphibians [52], we focused on examining a
150 potential role for miR-124 in regenerating neurons of the invertebrate, *Lymnaea*.

A. Novel

B. Mature

C.

microRNA	Upregulated in RA	Downregulated in RA
let-7		✓
let-7a	✓	
let-7d		✓
miR-96a	✓	
miR-96b		✓
miR-1994a	✓	
miR-1994b		✓
miR-281-3p		✓
miR-281-5p	✓	
bantam		✓
miR-8		✓
miR-9		✓
miR-125a		✓
miR-125b		✓
miR-317		✓
miR-745a		✓
miR-1985		✓
miR-2157		✓
miR-2715		✓
miR-3500		✓
miR-8456		✓
miR-2a	✓	
miR-2g	✓	
miR-2c	✓	
miR-29b	✓	
miR-124a	✓	
miR-124c	✓	
miR-182	✓	
miR-184b	✓	
miR-193	✓	
miR-216b	✓	
miR-279	✓	
miR-750	✓	
miR-1175	✓	
miR-1986	✓	
miR-2687	✓	
miR-8414	✓	
miR-9404	✓	

151

152 **Figure 2. Mature miRNAs that were differentially expressed between regenerating CNS
153 incubated in RA, or non-regenerating CNS incubated in EtOH. A)** Pie chart depicts the total
154 number of novel sequences identified by miRNA-Sequencing. Of these sequences, 38 exhibited at
155 least a 2-fold increase in CNS incubated in RA (red), while 48 displayed at least a 2-fold reduction in
156 RA-treated samples (white). **B)** Pie chart depicts the total number of mature miRNA sequences
157 identified by miRNA-Sequencing analysis. Of the identified sequences, a large proportion did not
158 exhibit differential expression between CNS incubated in RA and EtOH (black). However, a small
159 subset exhibited at least a 2-fold change between treatment groups and were either upregulated (red)
160 or downregulated (white) in RA-treated CNS. **C)** A complete list of differentially expressed mature
161 miRNAs following RA treatment. Table indicates the mature miRNA name and its corresponding
162 expression pattern in regenerating RA-treated CNS.

163

164 **Table 1.** Putative biological roles and mRNA targets of miRNAs that exhibited differential
165 expression following treatment with RA.

Biological role	Mature miRNA	Target	Reference
Tumorgenesis	let-7	Cdk4	[23]
		HMGA2	[24]
	miR-96	FOXO1	[25]
	miR-124	Cdk4	[26]
	miR-125	ErbB2	[27]
		ENPEP, CK2-α, CCNJ, MEGF9	[28]
	miR-182	BRCA1	[29]
	miR-193	ERBB4	[30]
Differentiation	let-7	RAS	[31]
	miR-29b	FBXO2	[32]
	miR-184	Saxophone	[33]
Proliferation	Bantam	hid	[34]
	miR-96	PTPN9	[35]
	miR-125	A20	[36]
	miR-182	FOXF2	[37]
	miR-184	Numbl	[38]
Apoptosis	miR-9	MTHFD2	[39]
	miR-29	FoxM1	[40]
	miR-96	FOXO1	[25]
	miR-182	FOXO1	[41]
	miR-193	MCL1	[42]
Cell cycle regulation	let-7	Cdc34	[43]
	Bantam	hid	[34]
	miR-182	c-Met	[44]

| Nervous system-specific role	Mature miRNA	Target	Source
Neuronal differentiation	miR-9	PTBP1	[45]
		Rap2a	[46]
	miR-124	PTBP1	[47]
		Rap2a	[46]
		Sox9	[48]
		JAG1	[49]
Neuronal lifespan	let-7	Chinmo	[50]
	miR-125	Chinmo	[50]
Neurite guidance	miR-9	Gsh2, Foxg1	[51]
	miR-124	coREST	[52]
	miR-125	Sema4d	[53]
Synaptogenesis	miR-8	Fasciclin III, Neuroglian	[54]
	miR-124	GluA2	[55]
		CREB	[56]

166

167 *2.3. miR-124 is highly enriched in the adult Lymnaea CNS*

168   In vertebrates, miR-124 has been characterized as a neuronally-enriched miRNA [61] that
169 contains multiple variants, including miR-124a, b, and c [62]. We obtained sequences for two
170 conserved subtypes of miR-124 in the *Lymnaea* CNS, miR-124a and miR-124c. However, the number
171 of reads for each variant was notably low (Figure 3A). Rather than focus on each individual subtype,
172 we instead characterized the entire miR-124 family of microRNAs (henceforth referred to as
173 miR-124).
174   PCR was used to determine whether miR-124 shared a similar neuronally-enriched expression
175 in *Lymnaea* as it does in vertebrates. Indeed, we found miR-124 was enriched in the CNS, but largely
176 absent or undetectable from other adult tissues, including the heart, albumen, prostate and buccal
177 mass (Figure 3B). We next determined whether this miRNA was developmentally regulated, as it is
178 in vertebrates. In vertebrates, miR-124 is shown to temporally increase in abundance throughout

179   development, until reaching maximal expression in the adult CNS [61,63,64]. To determine whether
180   the same is true in *Lymnaea*, we performed qPCR on developing *Lymnaea* embryos and compared
181   miR-124 expression levels to that of the adult CNS. In developing *Lymnaea* embryos, the first
182   neurons of the CNS are born approximately 4 days following egg laying [65,65]. In the days
183   following, ganglia begin to form and continue to increase in size until ~10 days, when the embryos
184   hatch [66]. As such, we examined miR-124 expression at 6, 8 and 10 days after egg laying, at stages
185   when the CNS has begun to develop [65,66]. miR-124 was expressed at low levels over the course of
186   *Lymnaea* development, and did not significantly increase in expression across these developmental
187   time points ($F_{(3,8)}$ = 17.63; P = 0.0007)(Figure 3C). However, miR-124 is more abundant in the adult
188   CNS, as shown in vertebrates [61,63,64] (Figure 3C), and was significantly higher than at 6
189   (p=0.0013), 8 (p=0.0014), and 10 days (p=0.0022) of development.
190   After confirming miR-124 was indeed a neuronally-enriched miRNA in adult *Lymnaea*, we next
191   used qPCR to confirm its differential expression between regenerating (RA-treated) and
192   non-regenerating (EtOH-treated) CNS. Although the mean relative level of expression of miR-124 in
193   RA-treated brains was ~ 25% greater than in those treated with EtOH, this difference approached,
194   but did not quite reach statistical significance (p=0.07; Figure 3D).

195
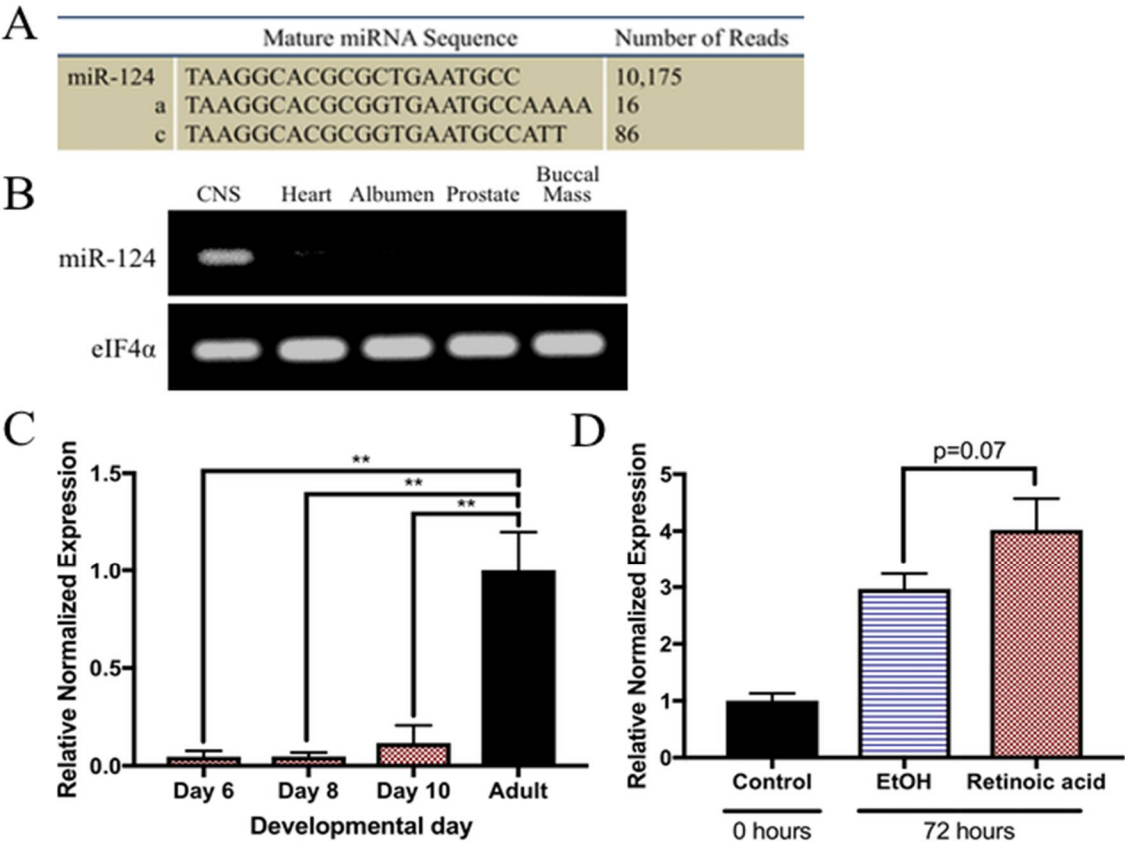
Figure 3. miR-124 expression in the adult *Lymnaea* CNS. A) Number of miR-124 sequence reads in
Lymnaea CNS, determined by miRNA-Sequencing. The family of miR-124 contains a and c subtypes
in low abundance. **B)** Tissue-specific expression of miR-124 in adult *Lymnaea*. PCR demonstrates that
miR-124 is enriched within the adult CNS, but appears diminished or completely undetectable in
other tissues. eIF4α was used as the positive loading control. **C)** miR-124 expression during *Lymnaea*
development. At 6, 8, and 10 days post egg laying, miR-124 expression remained relatively uniform,
and was not statistically significant across developmental days. However, miR-124 exhibited a
significant increase in the adult CNS in comparison to earlier developmental days (**= p<0.01). **D)**
miR-124 expression in the regenerating *Lymnaea* CNS. The mean relative normalized expression is
26% greater in RA-treated CNS, in comparison to EtOH controls. However, this increase did not
reach statistical significance (p=0.07). For RT-qPCR, data was made relative to the expression of the
acutely isolated CNS (control) and normalized to β-tubulin, actin, and eIF4α.

208   *2.4. miR-124 is expressed in both the Pedal and Right Parietal ganglia*

209   miRNAs are generally cell-type specific and importantly, have exhibited differential expression
210   patterns in specific regions within the CNS of both mice [67] and zebrafish [68]. Our next aim was to
211   determine whether specific patterns of expression of miR-124 exist within different ganglia of the
212   molluscan CNS. To this end, we utilized the Pedal ganglia and Right Parietal ganglion (Figure 4A),
213   which are known to contain different classes of motorneurons [69,70]. *In situ* hybridization indicated
214   a perinuclear distribution of miR-124 in cells of both the Pedal ganglia (Figure 4Bi) and the Right
215   Parietal ganglion (Figure 4Bii). Importantly, RT-qPCR analysis indicated that the overall expression
216   levels of miR-124 did not differ between these ganglia (p= 0.9535; Figure 4Biii).
217   A different miRNA, miR-133, has previously been shown to regulate RA-induced regeneration
218   of the newt spinal cord [14]. We thus also conducted *in situ* hybridization to examine its presence or
219   absence in these same ganglia. No detectable signal was obtained for miR-133 in either ganglion (Fig
220   4Ci,ii). miR-133 was however, detectable by RT-qPCR (Figure 4Ciii), which showed no difference in
221   expression across ganglia (p= 0.1862). These data also indicated very low expression levels of
222   miR-133, confirmed also by our miRNA-Sequencing results. Hence, no further analysis was
223   conducted for miR-133.

224
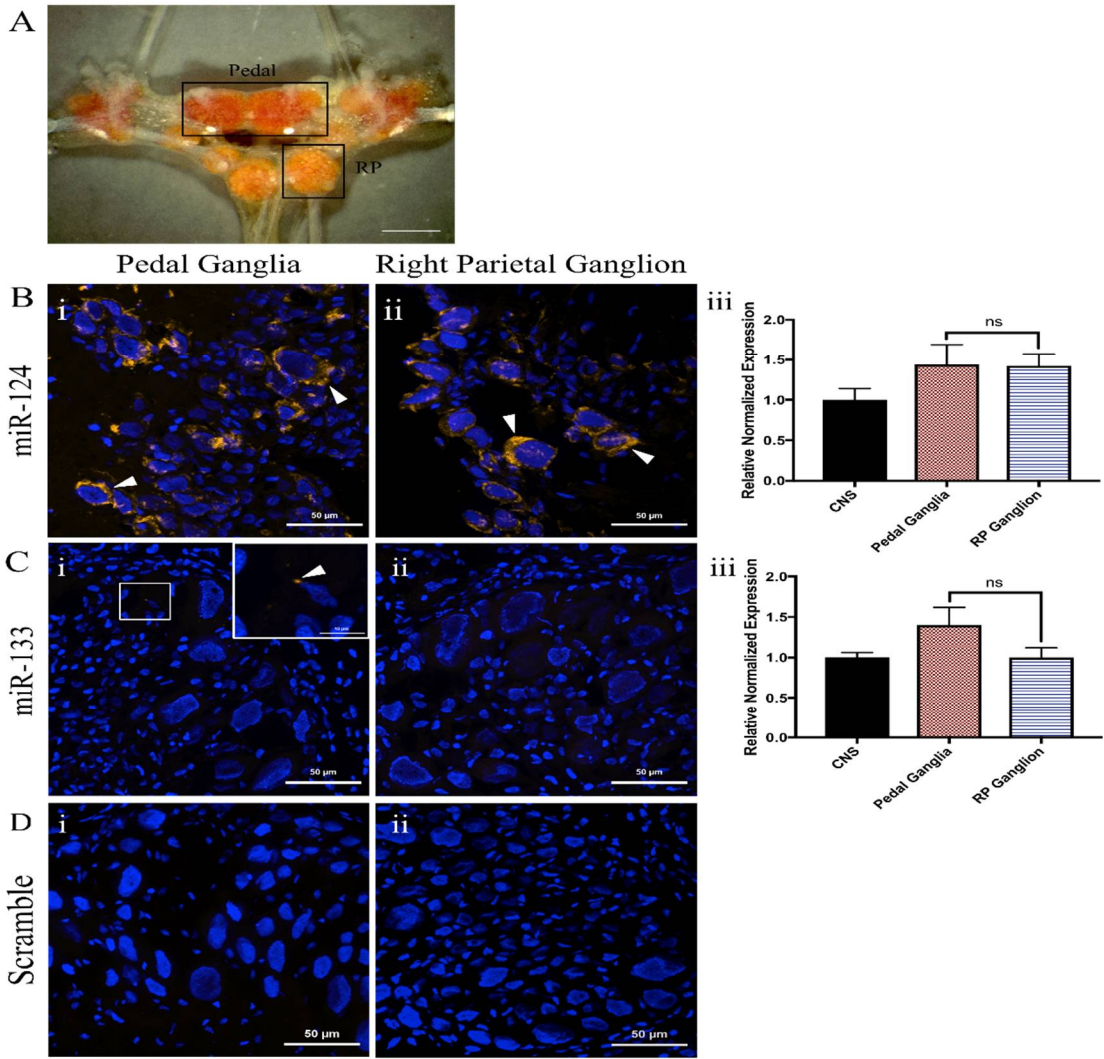
225   **Figure 4. Expression of microRNAs -124 and -133 in different ganglia of the *Lymnaea* CNS. A)**
226   Representative image of a *Lymnaea* CNS (Scale bar=1mm). Boxes represent different ganglia of the
227   CNS, including the Pedal ganglia and the Right Parietal (RP) ganglion. **B)** miR-124 demonstrates a
228   perinuclear distribution in both the Pedal (Bi) and Right Parietal (Bii) ganglia. Arrowheads indicate
229   representative areas of expression. RT-qPCR analysis demonstrates uniform expression across both

230   ganglia (Biii). **C)** Little to no miR-133 signal is detectable in either the Pedal ganglia (Ci), or the Right
231   Parietal ganglion (Cii). When examining miR-133 utilizing RT-qPCR, we detected similar expression
232   when comparing the Pedal and Right Parietal ganglia, however, this expression was minimal. For
233   RT-qPCR, data was made relative to the expression in the entire *Lymnaea* CNS, and normalized to
234   β-tubulin, actin, and eIF4α. **D)** Representative image of ganglia sections incubated with a scrambled
235   probe (negative controls). No signal was detected in either Pedal (Di) or Right Parietal (Dii) ganglia.
236   Scale bars (B-D) =50 μm.

237   *2.5. miR-124 is expressed within the cell bodies and neurites of two populations of regenerating motorneurons.*

238   We next examined miR-124 expression patterns within cultured, regenerating motorneurons
239   from both Pedal and Right Parietal ganglia. This examination of cultured cells allowed a better
240   resolution of cellular compartmentalization of the miRNA within regenerating neurons, and
241   provided more detailed information on cell-type-specific expression patterns. Importantly, different
242   functional classes of motorneurons were used. Pedal A (PeA) motorneurons innervate the cilia of the
243   foot musculature and are involved in locomotion [69]. These PeA ciliary motorneurons have
244   previously been shown to exhibit robust outgrowth and chemotropic responses upon application of
245   RA [10,18]. Another class of motorneuron, with as yet unknown responses to RA, were also
246   included; these Right Parietal A (RPA) motorneurons control movement of the pneumostome and
247   are thus required for aerial respiration [30].
248   In the cultured regenerating motorneurons (Figure 5A), miR-124 was consistently expressed
249   within the cell bodies of both PeA (n=46, Figure 5Bi) and RPA (n=41, Figure 5Bii) cell types. Once
250   again, miR-124 clearly exhibited a perinuclear distribution within the soma, similar to the expression
251   pattern we found in the ganglia. miR-124 was also detected within regenerating neurites of both PeA
252   (Figure 5Ci) and RPA motorneurons (Figure 5Cii). Interestingly, miR-124 was expressed as
253   individual punctae along the length of PeA and RPA neurites (Figure 5C). However, miR-124 was
254   not consistently expressed in all neurites of either cell type, with its expression in RPA neurites being
255   less frequent in comparison to PeA neurites (Figure 5C). Interestingly, miR-124 expression was often
256   abundant in branch points of both PeA (Figure 5Di) and RPA (Figure 5Dii) neurites.

257
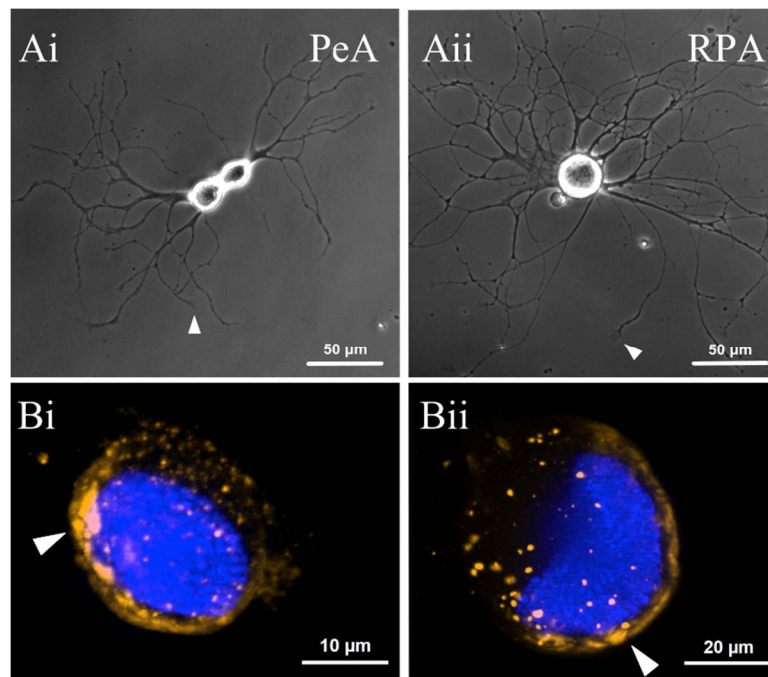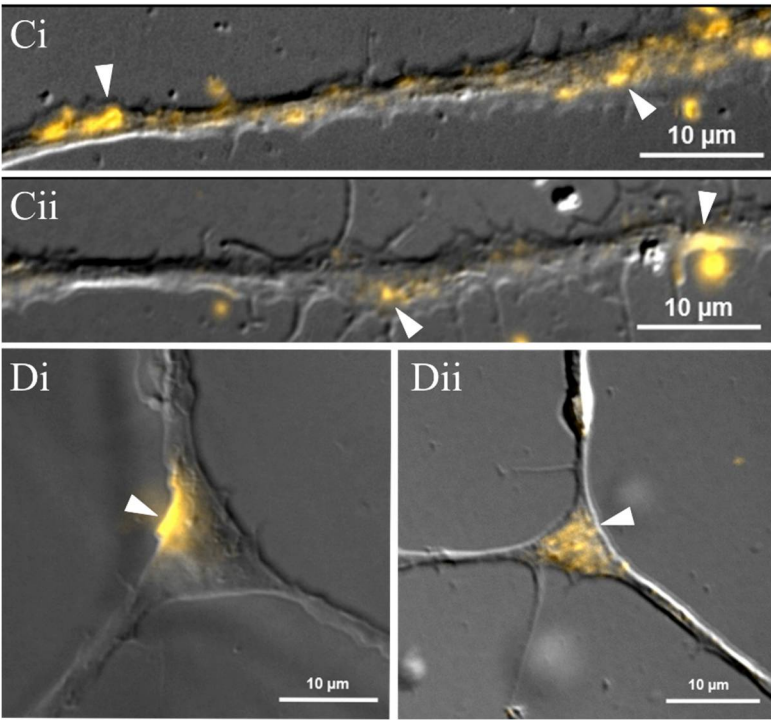
Figure 5. Expression of miR-124 in cultured regenerating motorneurons. A) Representative images of regenerating PeA (Ai) and RPA (Aii) neurons in culture. In each cell, extending neurites contain multiple branch points and numerous growth cones. White arrows indicate growth cones at the tip of neurites. **B)** miR-124 exhibits a perinuclear distribution (indicated by white arrowheads) within the soma of regenerating PeA (Bi) and RPA (Bii) motorneurons. **C)** Representative images of miR-124 expression along a PeA (Ci) and RPA (Cii) neurite. **D)** miR-124 appears to be localized in many (but not all) branch points of PeA (Di) and RPA (Dii) neurites.
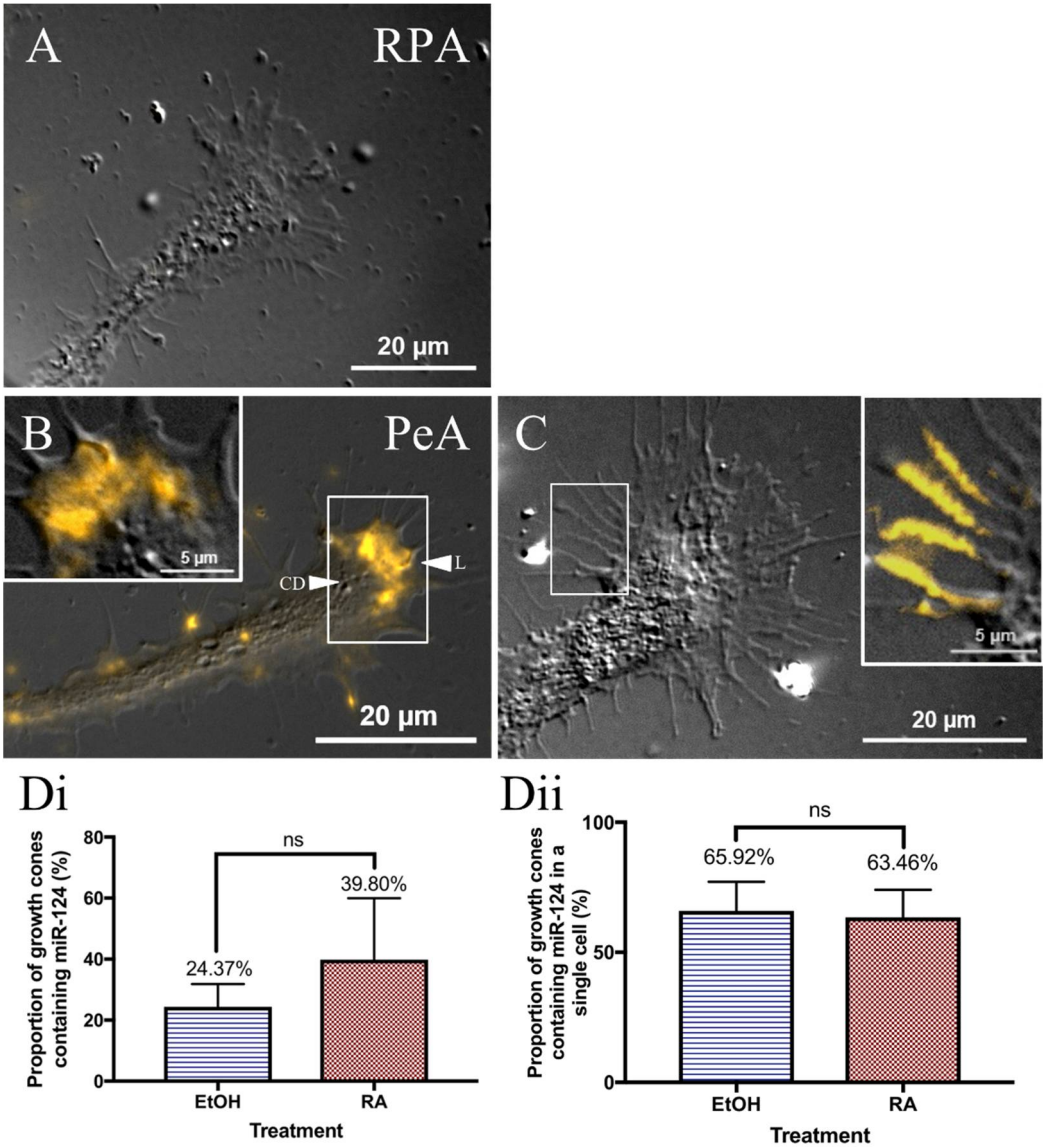
2.6. miR-124 is differentially expressed in the growth cones of different classes of motorneurons.

Neuronal growth cones are structures responsible for initiating and guiding regenerative outgrowth. We therefore next examined the expression of miR-124 within growth cones of the regenerating cultured RPA and PeA motorneurons. Interestingly, miR-124 was not detected in the growth cones of any RPA neurons (n = 0 of 43 growth cones; Figure 6A). It was however expressed within growth cones of PeA neurons (n = 28 growth cones). miR-124 was expressed along the leading edge of the PeA growth cones and was most frequently restricted to the lamellipodia (L; Figure 6B). It was, however, noticeably absent from the central domain (CD) of the growth cones (Figure 6B). miR-124 was also often associated or aligned with the filopodia in a long, fibrillar expression pattern (Figure 6C).

Interestingly, miR-124 was not expressed in all PeA growth cones. Therefore, we next determined whether exposure of regenerating neurites to retinoic acid might affect the expression pattern and/or number of growth cones expressing miR-124. Cultured PeA motorneurons were incubated in either RA (10^{-7}M) or in EtOH (0.001%; vehicle-control) during the first 12-18 hours of regenerating outgrowth. However, no significant differences in the proportion of growth cones containing miR-124 were shown between treatment groups (p=0.4995). miR-124 was found in the growth cones of ~ 40% of RA- treated neurons and ~ 25% of EtOH-treated neurons (Figure 6Di).

Cultured PeA motorneurons typically contain multiple neurites with numerous growth cones (see Figure 5Ai as an example). With this in mind, we re-examined the proportion of growth cones on individual motorneurons expressing miR-124, this time only analyzing those cells that expressed miR-124 in at least one of its growth cones. Once again, the proportion of growth cones that expressed this miRNA did not differ between cells treated with either RA (~63%) or EtOH (~66%) (p = 0.8747; Figure 6Dii).

289   In summary, these data demonstrate cell-type-specific expression of miR-124 in *Lymnaea*
290   growth cones and that this pattern of expression is not dependent on prior exposure to RA.

291

Figure 6. Differential expression of miR-124 in motorneuron growth cones. A) miR-124 is not
expressed in RPA growth cones (n=0 of 43). **B)** miR-124 is expressed along the leading edge within
the lamellipodia (L, arrowhead) of PeA growth cones, but is absent from the central domain (CD,
arrowhead). White box indicates area represented by inset image, magnified to show miR-124 in the
lamellipodia. **C)** miR-124 is also expressed in the filopodia of PeA growth cones. White box indicates
area represented by magnified inset image, demonstrating miR-124 within filopodia. **Di)** PeA cells
incubated in 0.001% EtOH or 10^{-7} M RA do not exhibit a significant difference in the proportion of
growth cones containing miR-124 (p=0.4995). ns= non-significant **Dii)** When a PeA cell contains
miR-124 in one of its growth cones, over 60% of the cell's remaining growth cones will also contain
miR-124 signal. This similar trend of expression is shown in cells incubated in both RA and EtOH.
No statistical significance (ns) was detected between treatment groups (p=0.8747).

3. Discussion

304   In this study, we performed the first transcriptome analysis of miRNAs expressed during CNS
305   regeneration in the invertebrate, *Lymnaea stagnalis. Lymnaea* is a useful model organism for the study
306   of adult CNS regeneration due to its extensive regenerative capacity, and ease of isolation of large,
307   identifiable neurons for cell culture. We identified 483 miRNAs in the adult *Lymnaea* CNS, and

308 discovered a specific subset that may contribute to RA-induced regeneration. In particular, we
309 focused on one neuronally-enriched miRNA, miR-124. Using RT-qPCR, we confirmed the
310 up-regulation of miR-124 during regeneration, and utilizing *in situ* hybridization, found that it was
311 present within motorneurons. Interestingly, we found miR-124 was enriched in the growth cones of
312 PeA motorneurons, but was restricted to the cell bodies and/or neurites of RPA motorneurons.
313 Together, these data are suggestive of a role for miR-124 in RA-induced CNS regeneration.

314 *3.1. Lymnaea stagnalis miRNA Transcriptome*

315 Using miRNA-Sequencing, we identified a large subset of 483 miRNA sequences in the snail
316 CNS. Of these 483 identified sequences, 264 miRNAs were conserved in other molluscan species,
317 while 219 represented a group of unique miRNAs that may be *Lymnaea*-specific. Interestingly, the
318 number of novel miRNAs within the *Lymnaea* CNS was relatively high; representing 45% of all
319 sequenced reads. In comparison, in the regenerating axolotl tail, fewer than 12% of the total
320 sequences were identified as novel miRNAs [71]. Rather than reflecting an over-abundance of novel
321 *Lymnaea*-specific miRNA sequences, this finding may be due to the minimal sequence information
322 available for the molluscan miRNA transcriptome. We expect that these potential novel miRNAs
323 will be identified in other molluscan species as more sequence data becomes available.
324 Interestingly, many of these novel sequences were differentially regulated during
325 CNS-regeneration. Specifically, 86 novel miRNA sequences exhibited at least a 2-fold increase or
326 decrease in RA-treated CNS, corresponding to 39% of all the novel sequences. We found that many
327 of the known or characterized mature miRNAs that were differentially regulated, contributed to
328 similar biological processes, including neuronal differentiation, proliferation, neurite guidance, or
329 synaptogenesis. As such, we predict the differentially regulated novel sequences may contribute to
330 similar events during CNS regeneration. However, a majority of the novel miRNAs exhibited an
331 extremely low number of reads, generally much lower than miR-133 (which was undetectable by *in*
332 *situ* hybridization). With such low abundance, characterizing the specific functions of these novel
333 sequences will prove to be difficult, as they may be undetectable by most standard molecular
334 techniques.

335 *3.2. miR-124 Expression Patterns in Lymnaea CNS*

336 Using both miRNA-Sequencing and RT-qPCR analyses, we found miR-124 was abundant
337 within the adult *Lymnaea* CNS, and was up-regulated in regenerating CNS, implicating its potential
338 role in molluscan CNS regeneration. miR-124 is a well-characterized miRNA that is predominantly
339 expressed in neuronal cells, and regulates a variety of processes, including: neuronal differentiation
340 [47,48], neurite outgrowth [52], neuronal cell fate [47,61], and the transition from neural progenitors
341 to mature neurons [47]. Importantly, miR-124 has also been shown to regulate CNS regeneration in
342 flatworms of the class Turbellaria [72]. When miR-124 was inhibited during planarian brain
343 regeneration, this resulted in a significant reduction of dopaminergic and GABAergic neurons,
344 reducing the overall brain size [72]. Together with our data, these studies support a role for miR-124
345 in the regeneration of invertebrate nervous systems.
346 In mice, miR-124 expression is 100 times higher in the CNS than in other tissues [73], and
347 gradually increases in abundance in parallel with neuronal maturation [61]. We found similar trends
348 in *Lymnaea,* as miR-124 was enriched in the CNS, compared to other tissues and organs. Moreover,
349 we also discovered miR-124 exhibited very low levels of expression during *Lymnaea* development
350 but was highly enriched in the mature adult snail CNS. Collectively, these data indicate miR-124
351 shares similar expression patterns in an invertebrate species as it does in some vertebrates and is
352 highly enriched in the mature CNS.

353 *3.3. Expression of miR-124 in Motorneurons*

354 To further characterize miR-124 expression, we determined the subcellular distribution of
355 miR-124 within individual regenerating motorneurons, and specifically, within the growth cone.

356   The presence of miRNAs within neuronal growth cones has previously been indicative of their role
357   in controlling neurite outgrowth and growth cone guidance [52,74-76]. As such, miRNAs within the
358   growth cone can rapidly down-regulate mRNAs that might impede neurite sprouting or impede
359   specific turning responses. In *Xenopus laevis*, miR-124 is localized to the growth cones of retinal
360   ganglion cells, and regulates neurite outgrowth in response to the guidance cue, Sema3A [52].
361   Similarly, in our present study we discovered that miR-124 was expressed in the growth cones of
362   PeA ciliary motorneurons. Interestingly, we determined that the number of PeA growth cones
363   containing miR-124 was not significantly altered when cells were cultured in the presence of RA in
364   comparison to EtOH alone. This may indicate that miR-124 does not play an integral role in
365   RA-induced neurite sprouting. However, miR-124 may instead contribute to fast-acting growth cone
366   turning responses, similar to other vertebrate growth cone-specific miRNAs [52,74-76]. Within
367   vertebrate growth cones, miRNAs have been shown to regulate local protein synthesis to rapidly
368   alter cytoskeleton dynamics in response to specific guidance cues. In *Lymnaea*, when local protein
369   synthesis is inhibited in PeA growth cones, their attractive chemotropic response to RA is abolished
370   [18]. This may implicate miR-124 as a positive regulator of local mRNA translation during
371   fast-acting growth cone turning responses, as opposed to a substantial role in neurite sprouting.

372   Interestingly, we discovered that miR-124 did not share a similar expression pattern in the
373   growth cones of RPA motorneurons. miR-124 was expressed in ~40% of all PeA growth cones, but
374   completely absent in all RPA growth cones examined. This suggests that miR-124 may not be
375   involved in regulating growth cone guidance in all motorneuron cell types. Indeed, it is likely that
376   different miRNAs may mediate the turning behaviours of different classes of motorneurons,
377   possibly in response to a variety of guidance cues encountered during innervation of different
378   targets during development.

379   In this study, we detected miR-124 in the cell bodies of both populations of *Lymnaea*
380   motorneurons studied, though interestingly, it was not previously detected in motorneurons of
381   another molluscan species. In *Aplysia californica*, miR-124 was found to be an essential regulatory
382   molecule at the cultured sensory-motor synapses, where it regulated the transcription factor, CREB
383   [56]. miR-124 was, however, primarily expressed in the sensory neurons and was undetected in the
384   motorneurons [56]. However, the sensory and motorneurons were cultured together and formed
385   synaptic connections [56], which may have affected expression levels in either cell, compared to
386   neurons cultured in isolation. It is possible that miR-124 may exhibit a higher abundance in
387   motorneurons prior to detecting a synaptic partner. Alternatively, the expression of miR-124 may be
388   species-specific and/or cell-type specific. Due to the limited number of sensory neurons that have
389   been identified in *Lymnaea*, we did not compare the expression patterns of miRNA between sensory
390   and motorneurons in this study.

391   *3.4. Role of miR-124 During RA-Induced CNS Regeneration*

392   Using miRNA-Sequencing, we demonstrated that miR-124 was upregulated in RA-treated
393   CNS, a trend that has also been described in vertebrate cell cultures [58,59]. In *Lymnaea*, the
394   expression of both nuclear receptors that bind retinoic acid, RXR [19] and RAR [20], increase during
395   CNS development. Similarly, a specific RAR subtype, RARβ, has been shown to increase in a
396   stage-specific manner during CNS regeneration in the adult newt [13]. As both RXR and RAR are
397   likely critical during RA-induced regeneration [13,77], and expressed in *Lymnaea* PeA growth cones
398   [19,20], it is possible that miR-124 could be targeting either mRNA sequence during specific stages of
399   regeneration. Indeed, the 3'UTR of the *Lymnaea* RAR and RXR mRNAs contain potential binding
400   sites for miR-124, though we have not yet explored whether these mRNAs are found locally in the
401   neurites and/or growth cones. Interestingly, during newt spinal cord regeneration, RARβ protein
402   increases [13], while RXR is instead downregulated [77]. If similar trends are exhibited during
403   invertebrate CNS regeneration, it is feasible that *Lymnaea* RXR may act as a potential target for
404   miR-124 during *Lymnaea* CNS-regeneration.

405   Alternatively, miR-124 may target mRNAs responsible for degradation of RA. Specifically,
406   Cytochrome P450 protein 26 (Cyp26) is responsible for degrading all-*trans* RA, and is expressed in

407 *Lymnaea* (Genbank Accession No. KF669878). Indeed, the 3'UTR of the *Lymnaea* Cyp26 mRNA
408 contains multiple binding sites for miR-124, suggesting this mRNA may also act as a potential
409 binding site for miR-124 during RA-induced regeneration. However, its presence within PeA or RPA
410 neurites and growth cones has not yet been determined. Alternatively, miR-124 may target mRNAs
411 that may impede neuronal outgrowth. However, as the *Lymnaea* genome has not yet been
412 sequenced, it is difficult to obtain an exhaustive list of potential *Lymnaea* mRNA targets for miR-124
413 at this time.
414   In summary, this study provides the first miRNA-Sequencing analysis of miRNAs in the
415 regenerating CNS of the mollusc, *Lymnaea stagnalis* and more importantly, characterizes classes of
416 both novel and conserved miRNAs that are regulated during RA-induced regeneration of the adult
417 CNS in this invertebrate. We also demonstrate that a specific, conserved miRNA, miR-124, is
418 abundant in the adult snail CNS, as it is in vertebrates. Furthermore, we provide new evidence for
419 cell-type specific expression of miR-124 in the growth cones of different classes of motorneurons. In
420 future studies, it will be important to characterize the expression patterns and potential targets of
421 our other miRNAs whose expression is mediated by RA signaling, and to identify mRNA targets
422 and functions of these miRNAs during CNS regeneration.

423 **4. Methods**

424 *4.1. Isolation of CNS*

425   *Lymnaea stagnalis* were bred in the laboratory and kept in aerated pond water at room
426 temperature on a 12hr:12hr light-dark cycle. For all experimental procedures, adult snails were
427 anesthetised in 25% Listerine® (containing menthol; 0.042% w/v) in pond water prior to removal of
428 the central ring ganglia (CNS).

429 *4.2. Regenerating CNS Preparation*

430   Isolated *Lymnaea* CNS were incubated in 3mL of defined medium (DM) containing 10^{-5}M RA (to
431 induce neural regeneration / neurite sprouting) in a plastic Falcon dish (VWR) for 72 hours. Different
432 CNS were also incubated in 0.1% EtOH as a vehicle control. Following the 72 hour incubation
433 period, any neurite sprouting from individual nerves emanating from the CNS were imaged using
434 Q-Capture imaging software.

435 *4.3. RNA-Sequencing of Lymnaea miRNAs*

436   RA-treated (regenerating) and EtOH-treated (non-regenerating) samples were collected by
437 pooling five-CNS from adult *Lymnaea* (shell length of 20-25 mm) per sample (1 biological replicate
438 was utilized). Total RNA was extracted using Tri-Reagent (Sigma) and Direct-zol RNA MiniPrep kit
439 (Zymo Research), and outsourced to LC Sciences (Houston, TX) for deep sequencing. A small RNA
440 library was generated from both regenerating and non-regenerating CNS samples using the
441 Illumina Truseq™ Small RNA Preparation kit, according to the manufacturer's instructions. This
442 generated library was utilized for cluster generation on Illumina's Cluster Station and sequencing on
443 Illumina GAIIx. Raw sequencing reads were obtained using Illumina's Sequencing Control Studio
444 software version 2.8 (SCS v2.8) following real-time sequencing image analysis and base-calling by
445 Illumina Real-Time Analysis version 1.8.70 (RTA v1.8.70).

446 *4.4. Isolation of Lymnaea embryos*

447   Egg masses were incubated in pond water at room temperature for 6, 8 and 10-days post egg
448 laying, corresponding to various stages of *Lymnaea* development (as described by Nagy and Elekes
449 [66]). At each developmental stage (day 6, 8, and 10) egg capsules were removed from their
450 gelatinous surroundings. Following isolation, all embryos encased in one egg mass were pooled and
451 frozen on liquid nitrogen for molecular analysis.

4.5. Cell Culture

Adult snails (16mm to 20mm in length) were used for all cell culture procedures. Following isolation of the *Lymnaea* CNS, individual ganglia were desheathed to expose cells of interest, including Pedal A (PeA) and Right Parietal A (RPA) motorneurons. Individually identified neurons were removed from the ganglia using suction applied via a fire polished pipette, and then plated on poly-L-lysine (Sigma) coated Falcon dishes (VWR). Culture dishes contained 3 mL of conditioned medium (CM), which contain unidentified trophic factors that can produce neurite outgrowth [18, 78]. In addition, 10^{-7}M RA was added to the culture dishes overnight to promote neurite sprouting [10,17]. All culture dishes were maintained at 21°C overnight. To determine the effects of RA on the proportion of growth cones expressing miR-124, cells were cultured in either 10^{-7}M RA or 0.001% EtOH (as the vehicle control).

4.6. RNA Isolation and cDNA synthesis

All *Lymnaea* organs and tissues were isolated from adult *Lymnaea stagnalis* with a shell length of 20-25mm, then immediately flash frozen on liquid nitrogen. For molecular analyses, one pooled sample for each organ contained: 2 CNS, 10 hearts, 10 albumen organs, 4 prostates, or 4 buccal masses. For analysis of individual CNS ganglia, the following were pooled for each sample: 20 Pedal ganglia, or 31 Right Parietal ganglia. For regenerating CNS samples, each biological replicate contained five pooled CNS. For all experiments, 3 biological replicates were utilized.

Total RNA was isolated from these samples using Tri-Reagent (Sigma) and Direct-zol RNA MiniPrep kit (Zymo Research). RNA quality was confirmed using spectrophotometry and gel electrophoresis. A total of 750 ng of RNA was utilized from each sample for cDNA synthesis using gene specific stem-loop primers with the SuperScript III Reverse Transcriptase kit (Invitrogen). Stem-loop primers were designed for miR-124 (RT:GTCGTATCCAGTGCAGGGTCCGAGGTATTCGCACTGGATACGACGGCATT) and miR-133 (RT: GTCGTATCCAGTGCAGGGTCCGAGGTATTCGCACTGGATACGACAGCTGG) based on sequences provided by RNA-Sequencing.

4.7. PCR

PCR reactions contained a total volume of 20 μL, consisting of 10x Taq buffer, 50 mM MgCl₂, 10mM dNTP mix (10mM each of dATP, dGTP, dCTP, and dTTP), iTAQ, both forward and reverse primers (10μM), template cDNA (750 ng), and nuclease-free water. Forward and reverse primers were as follows for miR-124: (F: GCCGCTAAGGCACGCG GTG; R: GTGCAGGGTCCGAGGT), miR-133: (F: GCCGCTTTGGTCCCCTTCA; R: GTGCAGGGTCCGAGGT), and eIF4α as a positive control: (F: CCGAGCGTGTAAGC AGCC; R: AGTTGTGGTTGACTTGCCAGAG). Thermal cycling parameters included an initial DNA denaturation step at 95°C for 3 minutes, then temperature cycling of 95°C for 30 s (denaturation), 55°C for 30 s (primer annealing), and 72°C for 1 minute (polymerase extension), and repeated for 40 cycles. End products combined with DNA loading dye were run on a 2.5% agarose gel and visualized using ethidium bromide staining.

4.8. RT-qPCR

Following cDNA synthesis, RT-qPCR was run using iQ SYBR Green Supermix (Bio-Rad) utilizing a CFX Connect Real-Time System (Bio-Rad). All samples were incubated for an initial DNA denaturation step for 3 minutes at 95°C, then underwent 40 thermo-cycles of 95°C for 30 s (DNA denaturation), 55°C for 1 minute (primer annealing) and 72°C for 1 minute (polymerase extension). Samples are reported relative to acutely isolated CNS, and normalized to β-tubulin (F: CATCCCCTAGCCATCTCTTCA; R: AGAGAGGCCTGGAGAGCT AA), actin (F: GCGATCTCACC GACTACCTG; R: ACGGACAATCTCACGCTCAG), and eIF4α (F: CCGAGCGTGTAAGCAGCC; R: AGTTGTGGTTGACTTGCCAGAG). Semi-quantitative analysis was performed utilizing the $\Delta\Delta C_T$ method, in accordance with the MIQE guidelines.

499   *4.9. LNA-FISH and Tyramide Signal Amplification*

500   Cultured cells or CNS were fixed in 4% paraformaldehyde for 20 minutes at room temperature,
501   then stored at 4°C in phosphate-buffered saline (PBS) until required. Prior to staining procedures,
502   both cells and CNS were treated with 3% H_2O_2 for 1h at room temperature to remove endogenous
503   peroxidase activity.
504   CNS were next washed, on rotation, with increasing sucrose concentrations: 10% for 30 min,
505   20% for 30 min, and 30% overnight at 4°C. Samples were then embedded in Optimal Cutting
506   Temperature (O.C.T.) compound (Tissue-Tek), and 12 μm sections were obtained using a cryostat
507   (Leica microsystems). Tissue sections were mounted on Superfrost Plus slides (Fisher Scientific).
508   For staining procedures, CNS tissue sections and cultured cells underwent the same procedures
509   modified from Lu and Tsourkas [79]. Samples were first washed in PBS, then dehydrated overnight
510   at 4°C in 70% ethanol. The next day, tissue sections and cells were incubated in hybridization buffer
511   (25% formamide, 0.05M EDTA, 4x Saline-Sodium Citrate (SSC) buffer, 10% dextran sulfate, 1x
512   Denharts solution, 0.5 mg/mL *E.Coli* tRNA, 20mM ribonucleoside vanadyl complexes, 9.2 mM citric
513   acid) at 58°C (for miR-124 and scramble) or 52°C (for miR-133) for 2 hours, then hybridized in 10 nM
514   of probe (Exiqon) for 1 hour at the same temperature. Samples next underwent stringency washes
515   with decreasing concentrations of SSC, including 4x SSC briefly, 2x SSC for 30 minutes, 1x SSC for 30
516   minutes, and 0.1% SSC for 20 minutes. Following these washes, cells and tissues were incubated in
517   blocking buffer (3% bovine serum, 4x SSC, 0.1% Tween-20) for 30 minutes, then horseradish
518   peroxidase (HRP)(Sigma) for 30 minutes at room temperature. Samples were next washed in TNT
519   buffer (0.1M Tris HCl, 0.15M NaCl, 0.05% Tween-20), then incubated in tyramide for 1 hour at room
520   temperature. Following a final series of washes in TNT buffer, all samples were mounted and
521   imaged using a Carl Zeiss Axio Observer.Z1 inverted light/epifluorescence microscope, with
522   ApoTome.2 optical sectioning.

523   *4.10. Statistics*

524   All data were analyzed utilizing Graphpad Prism, Version 7.0 for Mac OS X (La Jolla, CA, USA),
525   and values were expressed as the mean ± SEM. For statistical analysis investigating miR-124
526   expression during *Lymnaea* development, a one-way analysis of variance (ANOVA) was performed,
527   followed by Tukey's *post-hoc* test. For all other statistical analyses, a Students unpaired t-test was
528   performed. For all analyses, a P value less than 0.05 was considered to be statistically significant.

529   **Supplementary Materials:** None

534   **Author Contributions:** All authors contributed significantly to the production of this manuscript.
535   Contributions included: **Conceptualization,** RLC, GES, SEW; **Methodology,** SEW, GES, RLC, AN;
536   **Investigation,** SEW; **Resources,** RLC, GES, AN; **Data Curation,** SEW, GES; **Writing-Original Draft,** SEW;
537   **Writing- Review and Editing,** RLC, GES, AN; **Funding Acquisition,** RLC, GES

538   **Conflicts of Interest:** The authors declare no conflict of interest.

References

540   1.   Allison, P.; Benjamin, PR. Anatomical studies of central regeneration of an identified molluscan
541   interneuron. *Proceedings of the Royal Society B*. **1985,** doi: 10.1098/rspb.1985.0088.
542   2.   Cebria, F. Regenerating the central nervous system: How easy for planarians! *Development Genes and
543   Evolution*, **2007**, 217, 733-748.
544   3.   Tessier-Lavigne, M.; Goodman, C.S. The molecular biology of axon guidance. *Science,* **1996,** 274,
545   1123-1133.
546   4.   Sanchez Alvarado, A.; Tsonis, P.A. Bridging the regeneration gap: Genetic insights from diverse animal
547   models. *Nature Reviews*, **2006,** 7, 873-884.

5. Somorjai, I.M.; Somorjai, R.L.; Garicia-Fernandez, J.; Escriva, H. Vertebrate-like regeneration in the invertebrate chordate amphioxus. *PNAS,* **2012,** 109, 517-522

6. Maden, M.; Gale, E.; Kostetskii, I.; Zile, M. Vitamin A-deficient quail embryos have half a hindbrain and other neural defects. *Current Biology,* **1996,** 6, 417-426.

7. Maden, M. Role and distribution of retinoic acid during CNS development. *International Review of Cytology,* **2001,** 209, 1-77.

8. Maden, M. Retinoic acid in development and regeneration. *Journal of Biosciences,* **1996,** 21, 299-312.

9. Dmetrichuk, J.M.; Spencer, G.E.; Carlone, R.L. Retinoic acid-dependent attraction of adult spinal cord axons towards regenerating newt limb blastemas in vitro. *Developmental Biology,* **2005,** 281, 112-120.

10. Dmetrichuk, J.M.; Carlone, R.L.; Spencer, G.E. Retinoic acid induces neurite outgrowth and growth cone turning in invertebrate neurons. *Developmental Biology,* **2006,** 294, 39-49.

11. Hunter, K.; Maden, M.; Summerbell, D.; Eriksson, U.; Holder, N. Retinoic acid stimulates neurite outgrowth in the amphibian spinal cord. *PNAS,* **1991,** 88, 3666-3670.

12. Prince, D.J.; Carlone, R.L. Retinoic acid involvement in the reciprocal neurotrophic interactions between newt spinal cord and limb blastemas in vitro. *Developmental Brain Research,* **2003,** 140, 67-73.

13. Carter, C.; Clark, A.; Spencer, G.; Carlone, G. Cloning and expression of a retinoic acid receptor β2 subtype from the adult newt: Evidence for an early role in tail and caudal spinal cord regeneration. *Developmental Dynamics,* **2011,** 240, 2613-2625

14. Lepp, A.; Carlone, R. RARβ2 expression is induced by the down-regulation of microRNA 133a during caudal spinal cord regeneration in the adult newt. *Developmental Dynamics,* **2014,** doi: 10.1002/dvdy.24210.

15. Lepp, A.; Carlone, R. MicroRNA dysregulation in response to RARβ2 inhibition reveals a negative feedback loop between microRNAs 1, 133a, and RARβ2 during tail and spinal cord regeneration in the adult newt. *Developmental Dynamics,* **2015,** 244, 1519-1537.

16. Yu, Y.M.; Gibbs, K.M.; Davila, J.; Campbell, N.; Sung, S.; Todorova, T.I.; Otsuka, S.; Sabaawy, H.E.; Hart, R.P.; Schachner, M. 2011. MicroRNA miR-133b is essential for functional recovery after spinal cord injury in adult zebrafish. *European Journal of Neuroscience,* **2011,** 33, 1587–1597

17. Dmetrichuk, J.M.; Carlone, R.L.; Jones, T.R.B.; Vesprini, N.D.; Spencer, G.E. Detection of endogenous retinoids in the molluscan CNS and characterization of the trophic and tropic actions of 9-cis retinoic acid on isolated neurons. *Journal of Neuroscience,* **2008,** 28, 13014-13024.

18. Farrar, N.R.; Dmetrichuk, J.M.; Carlone, R.L.; Spencer, G.E. A novel, nongenomic mechanism underlies retinoic acid-induced growth cone turning. *Journal of Neuroscience,* **2009,** 29, 14136-14142.

19. Carter, C.J.; Farrar, N.; Carlone, R.L.; Spencer, G.E. Developmental expression of a molluscan RXR and evidence for its novel, nongenomic role in growth cone guidance. *Developmental Biology,* **2010,** 343, 124-137.

20. Carter, C.J.; Rand, C.; Mohammad, I.; Lepp, A.; Vesprini, N.; Wiebe, O.; Carlone, R.; Spencer, G.E. Expression of a retinoic acid receptor (RAR)-like protein in the embryonic and adult nervous system of a protostome species. *Journal of Experimental Zoology,* **2015,** 324B, 51-67.

21. Starega-Roslan, J.; Krol, J.; Koscianska, E.; Kozlowski, P.; Szlachcic, W.J.; Sobczak, K.; Krzyzosiak, W.J. Structural basis of microRNA length variety. *Nucleic Acid Research,* **2011,** 39, 257-268.

22. Lagos-Quintana, M.; Rauhut, R.; Lendeckel, W.; Tuschl, T. Identification of novel genes coding for small expressed RNAs. *Science,* **2001,** 294, 853-858.

23. Schultz, J.; Lorenz, P.; Gross, G.; Ibrahim, S.; Kunz, M. MicroRNA let-7b targets important cell cycle molecules in malignant melanoma cells and interferes with anchorage-independent growth. *Cell Research,* **2008,** 18, 549-557.

24. Sun Lee, Y.; Dutta, A. The tumo suppressor microRNA let-7 represses the HMGA2 oncogene. *Genes & Development,* **2007,** 21, 1025-1030.

25. Guo, Y.; Liu, H.; Zhang, H.; Shang, C.; Song, Y. miR-96 regulates FOXO1-mediated cell apoptosis in bladder cancer. *Oncology Letters,* **2012,** 4, 561-565.

26. Feng, T.; Xu, D.; Tu, C.; Li, W.; Ning, Y.; Ding, J.; Wang, S.; Yuan, L.; Xu, N.; Qian, K.; Wang, Y.; Qi, C. miR-124 inhibits cell proliferation in breast cancer through downregulation of CDK4. Tumor Biology, **2015,** 38, 5987-5997.

27. Budd, WT.; Seashols-Williams, SJ.; Clark, GC.; Weaver, D.; Calvert, V.; Petricoin, E.; Dragoescu, EA.; O'Hanlon, K.; Zehner, ZE. Dual action of miR-125b as a tumor suppressor and oncomiR-22 promotes prostate cancer tumorigenesis. *PLoS One,* **2015,** 10(11).

28. Feliciano, A.; Castellvi, J.; Artero-Castro, A.; Leal, J.A.; Romagosa, C.; Hernandez-Losa, J.; Peg, V.; Fabra, A.; Vidal, F.; Kondoh, H.; Ramon Y Cajal, S.; Lleonart, ME. miR-125b acts as a tumor suppressor in breast cancer tumorgenesis via its novel direct targets ENPEP, CK2-α, CCNJ, and MEGF9. *PLoS One,* **2013**, 8.

29. Moskwa, P.; Buffa, F.M.; Pan, Y.; Panchakshari, R.; Gottipati, P.; Muschel, R.J.; Beech, J.; Kulshrestha, R.; Abdelmohsen, K.; Weinstock, D.M.; Gorospe, M.; Harris, A.L.; Helleday, T.; Chowdhury, D. miR-182-mediated downregulation of BRCA1 impacts DNA repair and sensitivity to PARP inhibitors. *Molecular Cell,* **2011**, 41, 210-220.

30. Liang, H.; Liu, M.; Yan, X.; Zhou, Y.; Wang, W.; Wang, X.; Fu, Z.; Wang, N.; Zhang, S.; Wang, Y.; Zen, K.; Zhang, C.Y.; Hou, D.; Li, J.; Chen, X. miR-193a-3p functions as a tumor suppressor in lung cancer by downregulation ERBB4. *Journal of Biological Chemistry*, **2014**, jbc-M114.

31. Johnson, S.M.; Grosshans, H.; Shingara, J.; Byrom, M.; Jarvis, R.; Cheng, A.; Labourier, E.; Reinert, K.L.; Brown, D.; Slack, F.J. RAS is regulated by the let-7 microRNA family. *Cell*, **2005**, 120, 635-647.

32. Cushing, L.; Crostinean, S.; Xu, W.; Jiang, Z.; Madden, L.; Kuang, P.; Huang, J.; Weisman, A.; Hata, A.; Croce, C.M.; Lu, J. Disruption of miR-29 leads to aberrant differentiation of smooth muscle cells selectively associated with distal lung vasculature. *PLoS Genetics*, **2015**, 11, e1005238.

33. Iovino, N.; Pane, A.; Gaul, U. miR-184 has multiple roles in Drosophila female germline development. *Developmental Cell*, **2009**, 17, 123-133.

34. Brennecke, J.; Hipfner, D.R.; Stark, A.; Russell, R.B.; Cohen, S.M. bantam encodes a developmentally regulated microRNA that controls cell proliferation and regulates the proapoptotic gene hid in Drosophila. *Cell,* **2003,** 113, 25-36.

35. Liu, M.; Wang, N.; Ye, C.; Zhao, C.; Liu, Y.; Fan, Q.; Zhang, C.Y.; Sang, J.; Zen, K.; Chen, X. miR-96 promotes cell proliferation, migration and invasion by targeting PTPN9 in breast cancer. *Scientific Reports*, **2016**, 6, 37421.

36. Hong, Y.; Liang, H.; Rehman, U.U.; Wang, Y.; Zhang, W.; Zhou, Y.; Chen, S.; Yu, M.; Cui, S.; Zheng, A.; Qu, J.Q.; Yi, H.M.; Ye, X.; Huang, W.; Xiao, T.; Li, J.Y.; Wang, Y.Y.; Feng, J.; Zhu, J.F.; Lu, S.S.; Yi, H.; Xiao, Z.Q. miR-125b regulates proliferation and apoptosis of nasopharyngeal carcinoma by targeting A20/NF-κB signaling pathway. *Cell Death and Disease*, **2017**, 8, e2855.

37. Zhang, X.; Ma, G.; Liu, J.; Zhang, Y. MicroRNA-182 promotes proliferation and metastasis by targeting FOXF2 in triple-negative breast cancer. *Oncology Letters*, **2017**, 14, 4805-4811.

38. Liu, C.; Teng, Z.Q.; Santistevan, N.J.; Szulwach, K.E.; Guo, W.; Jin, P.; Zhao, X. Epigenetic regulation of miR-184 by MBD1 governs neural stem cell proliferation and differentiation. *Cell Stem Cell*, **2010**, 6, 433-444.

39. Selcuklu S.D.; Donoghue M.T.; Rehmet K.; de Souza Gomes, M.; Fort, A.; Kovvuru, P.; Muniyappa, M.K.; Kerin, M.J.; Enright, A.J.; Spillane, C. MicroRNA-9 inhibition of cell proliferation and identification of novel miR-9 targets by transcriptome profiling in breast cancer cells. *Journal of Biological Chemistry*, **2012**, 287(35), 29516-29528.

40. Wang, X.; Zhong, H.; Wang, L.; Dong, Y.; Jia, A.; Mo, Q.; Zhang, C. miR-29 induced K562 cell apoptosis by downregulating FoxM1. *Medical Science Monitor*, **2015**, 21, 3115-3120.

41. Kim, K.M.; Park, S.J.; Jung, S.H.; Kim, E.J.; Jogeswar, G.; Ajita, J.; Rhee, Y.; Kim, C.H.; Lim, S.K. miR-182 is a negative regulator of osteoblast proliferation, differentiation, and skeletogenesis through targeting FoxO1. *Journal of Bone Mineral Research*, **2012**, 27, 1669-1679.

42. Nakano, H.; Yamada Y.; Miyazawa T.; Yoshida T. Gain-of-function microRNA screens identify miR-193a regulating proliferation and apoptosis in epithelial ovarian cancer cells. *International Journal of Oncology*, **2013**, 42, 1875-1882.

43. Legesse-Miller, A.; Elemento, O.; Pfau, S.J.; Forman, J.J.; Tavazoie, S.; Coller, H.A. let-7 overexpression leads to an increased fraction of cells in G2/M, direct down-regulation of Cdc34, and stabilization of Wee1 kinase in primary fibroblasts. *Journal of Biological Chemistry*, **2009**, 284, 6605-6609.

44. Kouri, F.M.; Hurley, L.A.; Daniel, W.L.; Day, E.S.; Hua, Y.; Hao, L.; Peng, C.Y.; Merkel, T.J.; Queisser, M.A.; Ritner, C.; Zhang, H.; James, C.D.; Sznajder, J.I.; Chin, L.; Giljohann, D.A.; Kessler, J.A.; Peter, M.E.; Mirkin, C.A.; Stegh, A.H. miR-182 integrates apoptosis, growth, and differentiation programs in glioblastoma. *Genes and Development*, **2015**, 29, 732-745.

45. Qi, X. The role of miR-9 during neuron differentiation of mouse retinal stem cells. *Artificial Cells, Nanomedicine, and Biotechnology*, **2016**, 44, 1883-1890.

46. Xue, A.; Yu, C.; Wang, Y.; Liu, L.; Zhang, K.; Fang, C.; Liu, F.; Bian, G.; Song, B.; Yang, A.; Ju, G.; Wang, J. miR-9 and miR-124 synergistically affect regulation of dendritic branching via the AKT/GSK3β pathway by targeting Rap2a. *Scientific Reports*, **2016**, 6.

47. Makeyev, E.V.; Zhang, J.; Carrasco, M.A.; Maniatis, T. The microRNA miR-124 promotes neuronal differentiation by triggering brain-specific alternative pre-mRNA splicing. *Molecular Cell*, **2007,** 27, 435-448

48. Cheng, L.C.; Pastrana, E.; Tavazoie, M.; Doetsch, F. miR-124 regulates adult neurogenesis in the subventricular zone stem cell niche. *Nature Neuroscience*, **2009**, 12, 399-408.

49. Liu, X.S.; Chopp, M.; Zhang, R.L.; Tao, T.; Wang, X.L.; Kassis, H.; Hozeska-Solgot, A.; Zhang, L.; Chen, C.; Zhang, Z.G. MicroRNA profiling in subventricular zone after stroke: miR-124a regulates proliferation of neural progenitor cells through Notch signaling pathway. *PLoS One,* **2011**, 6.

50. Chawla, G.; Deosthale, P.; Childress, S.; Wu, Y.C.; Sokol, N.S. A let-7-to-miR-125 microRNA switch regulates neuronal integrity and lifespan in Drosophila. *PLoS Genetics*, **2016**, 12(8): e1006247.

51. Shibata, M.; Nakao, H.; Kiyonari, H.; Abe, T.; Aizawa, S. MicroRNA-9 regulates neurogenesis in mouse telencephalon by targeting multiple transcription factors. *The Journal of Neuroscience*, **2011**, 31, 3407-3422.

52. Baudet, ML.; Zivraj, KH.; Abreu-Goodger, C.; Muldal, A.; Armisen, J.; Blenkiron, C.; Goldstein, LD.; Miska, EA.; Holt, CE. miR-124 acts through CoREST to control onset of Sema3A sensitivity in navigating retinal growth cones. *Nature Neuroscience,* **2011,** 15, 29-40.

53. Quiroz, J.F.D.; Tsai, E.; Coyle, M.; Sehm, T.; Echeverri, K. Precise control of miR-125b is required to create a regeneration-permissive environment after spinal cord injury. *Disease Models & Mechanisms*, **2014,** doi: 10.1242/dmm.014837.

54. Lu, C.S.; Zhai, B.; Mauss, A.; Landgraf, M.; Gygi, S.; Van Vactor, D. MicroRNA-8 promotes robust motor axon targeting by coordinate regulation of cell adhesion molecules during synapse development. *Philosophical Transactions of The Royal Society,* **2014**, 369.

55. Hou, Q.; Ruan, H.; Gilbert, J.; Wang, G.; Ma, Q.; Yao, W.D.; Man, H.Y. MicroRNA miR124 is required for the expression of homeostatic synaptic plasticity. *Nature Communications*, **2015**, 6.

56. Rajasethupathy, P.; Fiumara, F.; Sheridan, R.; Betel, D.; Puthanveettil, S.V.; Russo, J.J.; Sander, C.; Tuschi, T.; Kandel, E. Characterization of small RNAs in *Aplysia* reveals a role for miR-124 in constraining synaptic plasticity through CREB. *Neuron*, **2009,** 63, 803-817.

57. Maden, M. Retinoic acid in the development, regeneration and maintenance of the nervous system. *Nature Reviews*, **2007,** 8, 755-765.

58. Sempere, L.F.; Freemantle, S.; Pitha-Rowe, I.; Moss, E.; Dmitrovsky, E.; Ambros, V. Expression profiling of mammalian microRNAs uncovers a subset of brain-expressed microRNAs with possible roles in murine and human neuronal differentiation. *Genome Biology*, **2004**, 5, R13.

59. Annibali, D.; Gioia, U.; Savino, M.; Laneve, P.; Caffarelli, E.; Nasi, S. A new module in neural differentiation control: Two microRNAs upregulated by retinoic acid, miR-9 and -103, target the differentiation inhibitor ID2. *PloS One*, **2012.**

60. Yu, J.Y.; Chung, K.H.; Deo, M.; Thompson, R.; Turner, D.L. MicroRNA miR-124 regulated neurite outgrowth during neuronal differentiation. *Experimental Cell Research,* **2008,** 314, 2618-2633.

61. Smirnova, L.; Grafe, A.; Seiler, A.; Schumacher, S.; Nitsch, R.; Wilczyn, F.G. Regulation of miRNA expression during neural cell specification. *European Journal of Neuroscience,* **2005**, 21, 1469-1477.

62. Griffiths-Jones, S. miR-Base: The microRNA Sequence Database. *MicroRNA Protocols*, **2006**, 129-138.

63. Deo, M.; Yu, J.Y.; Chung, K.H.; Tippens, M.; Turner, D.L. Detection of mammalian microRNA expression by in situ hybridization with RNA oligonucleotides. *Developmental Dynamics*, **2006**, 235, 2538-2548.

64. Krichevsky, A.M.; Sonntag, K.C.; Isacson, O.; Kosik, K.S. Specific microRNAs modulate embryonic stem cell-derived neurogenesis. *Stem Cells*, **2006**, 24, 857-864.

65. Croll, R.P.; Voronezhskaya, E.E. Early elements in gastropod neurogenesis. *Developmental Biology*, **1996**, 173, 344–347.

66. Nagy, T.; Elekes, K. Embryogenesis of the central nervous system of the pong snail Lymnaea stagnalis L. An ultrastructural study. *Journal of Neurocytology*, **2000**, 29, 43-60.

67. Bak, M.; Silahtaroglu, A.; Moller, M.; Christensen, M.; Rath, M.F.; Skryabin, B. Tommerup, N.; Kauppinen, S. MicroRNA expression in the adult mouse central nervous system. *RNA*, **2008,** 14, 432-444.

68. Wienholds, E.; Kloosterman, W.P.; Miska, E.; Alvarez-Saavedra, E.; Berezikov, E.; de Bruijn, E.; Horvitz, H.R.; Kauppinen, S.; Plasterk, R.H. MicroRNA expression in zebrafish embryonic development. *Science*, **2005**, 309, 310-311.

69. Syed, N.I.; Winlow, W. Morphology and electrophysiology of neurons innervating the ciliated locomotor epithelium in Lymnaea stagnalis (L.). *Comparative Biochemistry and Physiology Part A: Physiology*, **1989**, 93, 633-644.

70. Magoski, NS. Syed, NI. Bulloch, AG. A neuronal network from the mollusc Lymnaea stagnalis. *Brain Research*, **1994**, 645, 201-214.

71. Gearhart, M.D.; Erikson, J.R.; Walsh, A.; Echeverri, K. Identification of conserved and novel microRNAs during tail regeneration in the Mexican Axolotl. *International Journal of Molecular Science*, **2015**, 16, 22046-22061.

72. Sasidharan, V.; Marepally, S.; Elliots, S.A.; Baid, S.; Lakshmanan, V.; Nayyar, N. Bansal, D.; Sanchez Alvarado, A.; Kumar Vemula, P.; Palakodeti, D. The miR-124 family of microRNAs is crucial for regeneration of the brain and visual system in the planarian Schmidtea mediterranea. *Development*, **2017**, 144, 3211-3223.

73. Mishima, T.; Mizuguchi, Y.; Kawahigashi, Y.; Takizawa, T.; Takizawa, T. RT-PCR-based analysis of microRNA (miR-1 and -124) expression in mouse CNS. *Brain Research*, **2007**, 1131, 37-43.

74. Han, L.; Wen, Z.; Lynn, R.C.; Baudet, M.L.; Holt, C.E.; Sasaki, Y.; Bassell, G.J.; Zheng, J.Q. Regulation of chemotropic guidance of nerve growth cones by microRNA. *Molecular Brain*, **2011**, 4.

75. Hancock, M.L.; Preitner, N.; Quan, J.; Flanagan, J.G. MicroRNA-132 is enriched in developing axons, locally regulated Rasa1 mRNA, and promotes axon extension. *The Journal of Neuroscience*, **2014**, 34, 66-78.

76. Bellon, A.; Iyer, A.; Bridi, S.; Lee, F.C.Y.; Ovando-Vazquez, C.; Corradi, E.; Longhi, S.; Roccuzzo, M.; Strohbuecker, S.; Naik, S.; Sarkies, P.; Miska, E.; Abreu-Goodger, C.; Holt, C.E.; Baudet, M.L. miR-182 regulated Slit2-mediated axon guidance by modulating the local translation of a specific mRNA. *Cell Reports*, **2017**, 18, 1171-1186.

77. Walker, S.E.; Nottrodt, R.; Maddalena, L.; Carter, C.; Spencer, G.E.; Carlone, R.L. Retinoid X receptor α downregulation is required for tail and caudal spinal cord regeneration in the adult newt. *Neural Regeneration Research*, **2018**, 13, 1036-1045.

78. Wong, R.G.; Hadley, R.D.; Kater, S.B.; Hauser, G.C. Neurite outgrowth in molluscan organ and cell cultures: The role of conditioning factor(s). *The Journal of Neuroscience*, **1981**, 1, 1008-1021.

79. Lu, J.; Tsourkas, A. Quantification of miRNA abundance in single cells using locked nucleic acid-FISH and enzyme-labeled fluorescence. In *Molecular Imaging*, Khalid Shah, Humana Press, Totowa, NJ, **2011**, 680, pp. 77-88.